Low Iris and Anterior Chamber Volume Associated with Deepening after Laser Peripheral Iridotomy in Primary Angle Closure Suspects

Hamed Esfandiari,[1,2] Nassim Amouhashemi,[1] Mehdi Yaseri,[3] Pooya Torkian,[1] Mohammad Pakravan,[4] Khosrow Jadidi,[5] Nils A Loewen[2*]

[1] Ophthalmic Research Center, Shahid Beheshti University of Medical Sciences, Tehran, Iran
[2] Department of Ophthalmology, School of Medicine, University of Pittsburgh, Pittsburgh, Pennsylvania, United States
[3] Department of Epidemiology and Biostatistics, School of Public Health, Tehran University of Medical Sciences, Tehran, Iran
[4] Ophthalmic Epidemiology Research Center, Shahid Beheshti University of Medical Sciences, Tehran, Iran
[5] Department of Ophthalmology, Baqiyatallah University of Medical Sciences, Tehran, Iran

*Correspondence: Nils A. Loewen, loewen.nils@gmail.com

Abstract

Purpose: To evaluate the association between baseline ocular variables and the opening of the anterior chamber angle by laser peripheral iridotomy (LPI) in primary angle closure suspects (PACS) using a new Fourier-domain swept-source anterior segment optical coherence tomography (FD-ASOCT).

Method: Sixty-six PACS eyes of 41 individuals were included in this prospective interventional case series. An FD-ASOCT (Casia SS-1000 OCT; Tomey, Nagoya, Japan) was used to measure biometric baseline variables and at one month after the LPI. Paired t-test was used to compare the difference between pre-and post-LPI measurements. Multivariate regression analysis was used to test for an association between baseline iris thickness and volume, anterior chamber depth and volume, and lens vault with a widening of the angle after an LPI.

Results: The mean age of participants was 58.6 ± 8.7 years, 682% of whom were female. The angle opening distance, recess area and trabecular iris surface area at 500 microns increased by 48 to 73% (all $p<0.001$). Lens vault and iris volume did not change. A low anterior chamber volume and low iris volume were associated with angle greater deepening by LPI.

Conclusion: Eyes with a shallow anterior chamber and thinner irises are more likely to experience angle opening from a LPI.

Keywords: primary angle closure suspect; laser peripheral iridotomy, swept source anterior segment OCT; anterior chamber volume, iris volume, CASIA OCT.

Introduction

Primary Angle Closure Glaucoma (PACG) is a major cause of vision loss around the word and in Asia in particular.[1] PACG has the highest prevalence in in East Asia (1.1%)[2] compared to only 0.4% in Iran,[3] which is more similar to Caucasian populations.[2] The anatomical features considered to put an eye at risk of angle closure are a crowded anterior segment and narrow anterior chamber angle which are often associated with a small corneal diameter, a short axial length, a shallow anterior chamber, a thick lens and iris, lens vault.[2,4–1011] Laser peripheral iridotomy (LPI) is a relatively safe procedure that helps reverse appositional angle closure, thereby relieving pupillary block, widening the angle and preventing optic nerve damage from increased intraocular pressure.[12–16] However, 60% of patients treated with an LPI continue to have some degree of angle closure.[15,17–19] Because the indication for an LPI is quite subjective and the number of PACS patients so large, treating everybody would pose serious challenges and not be cost-effective. Moreover, despite being a relatively low risk procedure, the risk of cataract development and endothelial cell loss has not been evaluated in long-term prospective studies.[20–22] The value of iris thickness, anterior chamber depth, iris curve, and lens vault to predict a successful LPI has previously been found to be relatively low.[13,23,24]

In the present study, we used a new Fourier-domain swept-source anterior segment OCT (FD-ASOCT; Casia SS-1000 OCT; Tomey, Nagoya, Japan) with a high scan speed (30 000 A-scans per second) that allows to image the angle by 128 cross-sections in less than 3 seconds. We hypothesized that this FD-ASOCT would allow for a more accurate assessment of anterior chamber baseline variables that predict widening of the anterior chamber angles following an LPI.

Methods

Study Design

This study was approved by ethics committee of Shahid Beheshti University of Medical Sciences and carried out in accordance with tenets of the Declaration of Helsinki. A total of 72 eyes of 43 consecutive Caucasian individuals with PACS were included from the general ophthalmology clinic between March 2014 to April 2015. Written informed consent was obtained from all participants. Inclusion criteria were angle closure on gonioscopic exam by Shaffer gonioscopic criteria with a scleral spur visibility score (SSVS) of at least 1 in each angle (described below) and age above 18 years. Exclusion criteria were peripheral synechiae, an intraocular pressure above 21 mmHg, a corneal opacity that would interfere with the image acquisition, signs of glaucomatous optic neuropathy, and any systemic condition or use of anticoagulants that could increase the risk of bleeding. Diagnosis of PACS, PAC, and PACG was based on the criteria established by the International Society of Geographic and Epidemiologic Ophthalmology (ISGEO).[25] PACS was defined as an eye in which the posterior trabecular meshwork was not seen over 270 degrees or more of the angle circumference on gonioscopy. PAC was defined using PACS criteria plus PAS reaching the scleral spur or beyond; evidence of prior acute IOP elevation, including iris atrophy, glaukomflecken, a dilated nonreactive pupil; or elevated IOP without signs of glaucomatous damage. PACG was defined by PAC and glaucomatous optic neuropathy or visual field defects.

At baseline, all patients underwent a comprehensive ophthalmic examination by an experienced glaucoma specialist including determination of best corrected visual acuity (BCVA), slit-lamp examination (Haag-Streit, Bern, Switzerland), Goldmann applanation tonometry (model AT900, Haag-Streit), gonioscopy with a Zeiss-style 4-mirror lens (model OPDSG, Ocular Instruments, Inc., Bellevue, WA), fundus examination, and perimetry (Humphrey visual field analyzer; model 750; Carl Zeiss Meditec, Dublin, California, USA).

Gonioscopy was performed by a trained ophthalmologist (HE) at x16 magnification in a darkroom setting using the Shaffer gonioscopic classification as described in the following: an angle between the iris and the trabecular meshwork surface of 35° to 45° was graded 4, between 20° and 35° as grade 3, between 10° to 20° as grade 2, and less than 10° was classified as grade 1. Grade 0 was assigned if angle structures were not observed.[26] IOP was measured twice by the same ophthalmologist between 9 to 11 AM. The average of 2 reading was recorded as patient's IOP. If 2 IOPs were different by more than 2 mmHg, a third measurement was taken, and the median was recorded.

Swept-Source Anterior Segment Optical Coherence Tomography

The anterior chamber angle scan protocol of the Casia SS-1000 OCT (FD-ASOCT) was used to obtain a volume scan consisting of 128 radial scans, each 16 mm in length and 6mm in depth. Measurement were done in the dark (0.3 lux) while the individual was asked to fixate on an internal target for 2.4 seconds it took the acquisition to complete. Images with motion or lid artifacts were excluded. After the scleral spur was manually determined, the trabecular iris space area (TISA), the angle opening distance (AOD), and trabecular-iris angle (TIA) were measured by the instrument's software in the nasal and temporal quadrant. The scleral spur was identified in the FD-ASOCT image as a protrusion of sclera into the anterior chamber. When the scleral spur was clearly visible, a visibility score (SSVS) of 2 was denoted.[27] In case of no detectable scleral spur, SSVS was graded 0, while moderate clarity of the scleral spur was graded as 1.[27] A glaucoma specialist experienced with this method (MP) determined the scleral spur location for each image.

By definition, the AOD is the perpendicular distance between a point 500µm (AOD 500) or 750 µm (AOD 750) anterior to the scleral spur and the opposing iris. TISA is a trapezoidal area (TISA 500 or 750) bounded by the AOD 500 or 750, the anterior iris surface, the inner corneoscleral wall and the perpendicular distance between the scleral spur and the opposing iris. Angle recess area (in mm2) is defined as the triangular area (ARA 500 or 750) bounded by the AOD 500 or 750, the anterior iris surface and the inner corneoscleral wall.[28] Iris thickness was measured at 2000 µm from the scleral spur (IT2000). Since the peripheral iridotomies were created closer to the superior and temporal angles, only the nasal angles were analyzed. The iris volume, anterior chamber depth, and anterior chamber volume were also measured. These variables have shown to have low measurement variabilities.[29]

The anterior chamber depth was determined as axial distance from the corneal endothelium to the anterior lens surface. LV was defined as the perpendicular distance from the anterior lens surface to the horizontal line connecting the two scleral spurs.

Laser Peripheral Iridotomy Technique

All LPIs were performed by the same ophthalmologist (NA). Pupillary constriction was achieved with 2% pilocarpine, and topical tetracaine was applied to the eye for anesthesia. An Abraham iridotomy lens was used with hypromellose 2.5% ophthalmic lubricant solution (Goniovisc; HUB pharmaceuticals, Rancho Cucamonga, CA) as a coupling agent. A single 4 mJ shot was applied with a neodymium-doped yttrium aluminum garnet (YAG) laser operating at 946 nm (VISULAS YAG III Combi, Zeiss Meditec, Jena, Germany) was used initially to gauge the tissue response to achieve patency and enlargement of the iridotomy. An average of 15 shots was needed. The surgeon confirmed the patency of the LPI by transillumination. A drop of apraclonidine and betamethasone were applied before discharging the patient. All LPIs were created in the superotemporal location between the 10-11 and 1-2 o'clock positions on the right and left eyes, respectively. All patients were started on betamethasone four times a day for four days and reexamined two and four weeks after the procedure. At the follow up visit at four weeks, FD-ASOCT imaging was repeated and performed by the same operator, at the same time of the day, and with the same protocol.

Statistical Analysis

All data was computed as mean, standard deviation, median, and range. Differences in preoperative and postoperative measurements for AOD 500, AOD 750, TISA 500, TISA 750, ARA 500, ARA 750, TIA 500, TIA 750, LV, AC volume, iris thickness, and iris volume were compared by paired Student's t-tests. Univariate and multivariate linear regression models, the latter adjusted for age and sex were used to test for an association between the baseline measurements of the iris thickness, iris volume, LV, and ACV and the changes in AOD 500, AOD 750, TISA 500 and TISA 750. The significance was set at $P<0.05$ for this study. Among all the variables included in our study, the nasal AOD 500 produced the maximum sample size, which we used to compute the proper sample size. To have a power of 95% to detect a difference as large as 0.10 before and after LPI when the standard deviation of this change was calculated to be 0.15 based on a pilot study, a total sample size of 64 eyes would be needed. All statistical analysis performed by SPSS software (IBM Corp. Released 2016. IBM SPSS Statistics for Windows, Version 24.0. Armonk, NY: IBM Corporation).

Results

Seventy-two eyes of 43 consecutive patients with PACS were enrolled in this study. Six eyes were excluded due to poor visualization of the scleral spur in FD-ASOCT images. At the time of the imaging, none of the individuals was on pilocarpine or other systemic agents that could constrict or dilate the pupil. Data from 66 eyes of 41 patients (28 female, 13 male) was used for the final analysis. The mean age was 58.6 ± 8.7 years. Mean IOP at the time of presentation was 13 ± 2.7 mmHg and remained unchanged at one month (13.3 ± 2.1 mmHg) after the LPI ($P= 0.421$). Mean central corneal thickness was

538 ± 29 micrometer (Table 1). The mean pre-LPI gonioscopic angle width (Shaffer grade) was 0.72 ± 0.41, which increased significantly to 1.83 ± 0.71, one month after the LPI (P < 0.001).

AOD 500 (0.35 ± 0.14 vs. 0.46 ± 0.15 mm, P<0.001), TISA 500 (0.17 ± 0.12 vs. 0.18 ± 0.06 mm, P < 0.001), ARA 500 (0.22 ± 0.09 vs.0.27 ± 0.1 mm2, P<0.001), ACD (2.37 ± 0.29 vs 2.45 ± 0.37, P= 0.001), AC width (106.9 ± 26.4 vs 119.8 ± 25.6, <0.001) increased after LPI (Figure 3 and Supplementary Table 1). However, there was no significant change in LV (0.27 ± 0.18 vs.0.27 ± 0.19, P+ 0.761) and iris volume (28.4 ± 4.8 vs 28.6 ± 5, P= 0.755) (Figure 3). Baseline iris thickness measured 2 mm from the scleral spur was 459 ± 34 µm that changed insignificantly to 458 ± 35 µm one month post LPI (P= 0.071).

The multivariate linear regression model found a significant association between lower baseline anterior chamber volume and AOD 500, AOD 750, TISA 500, TISA 750 opening at 1-month post-LPI. (respective P values: 0.036, 0.048, 0.020, and 0.041, Table 2, Figure 1). The baseline iris volume was associated with a significant angle opening at AOD 500, TISA 500, and TISA 750 one month after the LPI (Ps= 0.022, 0.001, and 0.041, respectively; Table 2 and Figure 2). For each 0.01 microliter of lower preoperative iris volume, TISA 500 increased by one square micrometer more after LPI.

Discussion

Our study evaluated the association between anterior chamber baseline parameters and LPI responses in PACS eyes. We observed significant widening of the angle after LPI evidenced by gonioscopic exam an increase in ACV, ACD, AOD 250, AOD 500, AOD 750, TISA 500, TISA 750, ARA 750, and TIA. Our findings are comparable to other imaging studies that used anterior segment OCT to evaluate the changes.[3013,24,31,32]In contrast to the ASOCT used in those with 12 cross-sectional images, the FD-ASOCT used here can rapidly obtain 128 radial scans to compute the the iris and anterior chamber volumes. The novel finding of our study is the association between a lower baseline iris volume and an increased angle widening after an LPI as best seen in TISA 500. A low baseline anterior chamber volume was also associated with a more significant increase in AOD, ARA, TISA, and TIA one month post-LPI but a clinically useful prediction formula could not be derived.

A possible explanation for an inverse relationship between a thinner iris and an improved angle deeping after an LPI is how a thinner iris might be more prone to bulging forward during a relative pupillary block.[33] Two ASOCT studies have examined the relationship between pre-LPI iris thickness and the amount of angle opening after the LPI: How et al. showed there is positive association,[23] but Lee et al. found a negative relationship.[24] Both studies used an ASOCT that uses a single-A scan at 2 mm from the scleral spur. This method is influenced by the regional difference of the iris and may not be an accurate representation of the iris volume. Our use of an FD-ASOCT allowed us to measure the entire volume of the iris instead of its thickness at a single point. Thinner irises were found to have less collagen type 1 resulting in altered biomechanical behavior.[34]

The mean ACV in our study increased from 106.9 ± 26.4 to 119.8 ± 25.6 ml after LPI, consistent with previous reports, despite different methods.[35,36] Interestingly, we found that the central ACD increased by 50 micrometers, not enough to explain the observed increase in ACV, which has to be the result of a

flattened iris. It has been suggested that aqueous accumulates in the vitreous which pushes the lens forward during a pupillary block.[15] When the LPI resolves the pupillary block the posterior entrapment is resolved and the lens can move backwards.

AOD was a similar variable that was significantly impacted by the iris and anterior chamber volume but to a lesser extent. AOD treats the iris surface as a straight line[37] and is a less accurate way of measuring angle changes compared to TISA and AOD.[38]

Our study had several limitations. We included only PACS making it difficult to estimate how eyes with full angle closure might have responded but there is no difficulty setting the indication for treatment in eyes with an acute angle closure. The scleral spur could not be identified automatically. We tried to make the results less variable by only using one experienced glaucoma specialist.

In summary, our study showed that a lower iris and anterior chamber volume measured by swept source anterior segment OCT are associated with larger angle opening after LPI in PACS eyes. This may aid clinicians in making a decision whether an LPI should be attempted or a primary lens extraction might be indicated.

References

1. Sun X, Dai Y, Chen Y, et al. Primary angle closure glaucoma: What we know and what we don't know. Prog Retin Eye Res 2017;57:26–45.

2. Tham Y-C, Li X, Wong TY, et al. Global prevalence of glaucoma and projections of glaucoma burden through 2040: a systematic review and meta-analysis. Ophthalmology 2014;121:2081–2090.

3. Pakravan M, Yazdani S, Javadi M-A, et al. A population-based survey of the prevalence and types of glaucoma in central Iran: the Yazd eye study. Ophthalmology 2013;120:1977–1984.

4. Lowe RF. Aetiology of the anatomical basis for primary angle-closure glaucoma. Biometrical comparisons between normal eyes and eyes with primary angle-closure glaucoma. Br J Ophthalmol 1970;54:161–169.

5. Lee DA, Brubaker RF, Ilstrup DM. Anterior chamber dimensions in patients with narrow angles and angle-closure glaucoma. Arch Ophthalmol 1984;102:46–50.

6. Marchini G, Pagliarusco A, Toscano A, et al. Ultrasound biomicroscopic and conventional ultrasonographic study of ocular dimensions in primary angle-closure glaucoma. Ophthalmology 1998;105:2091–2098.

7. Tarongoy P, Ho CL, Walton DS. Angle-closure glaucoma: the role of the lens in the pathogenesis, prevention, and treatment. Surv Ophthalmol 2009;54:211–225.

8. Wang N, Ouyang J, Zhou W, et al. [Multiple patterns of angle closure mechanisms in primary angle closure glaucoma in Chinese]. Zhonghua Yan Ke Za Zhi 2000;36:46–51, 5, 6.

9. Congdon NG, Youlin Q, Quigley H, et al. Biometry and primary angle-closure glaucoma among Chinese, white, and black populations. Ophthalmology 1997;104:1489–1495.

10. Nongpiur ME, He M, Amerasinghe N, et al. Lens vault, thickness, and position in Chinese subjects with angle closure. Ophthalmology 2011;118:474–479.

11. Thomas R, George R, Parikh R, et al. Five year risk of progression of primary angle closure suspects to primary angle closure: a population based study. Br J Ophthalmol 2003;87:450–454.

12. Schwartz LW, Rodrigues MM, Spaeth GL, et al. Argon laser iridotomy in the treatment of patients with primary angle-closure or pupillary block glaucoma: a clinicopathologic study. Ophthalmology 1978;85:294–309.

13. Lei K, Wang N, Wang L, Wang B. Morphological changes of the anterior segment after laser peripheral iridotomy in primary angle closure. Eye 2007;23:345–350. Available at: [Accessed October 24, 2017].

14. McGalliard JN, Wishart PK. The effect of Nd:YAG iridotomy on intraocular pressure in hypertensive eyes with shallow anterior chambers. Eye 1990;4 (Pt 6):823–829.

15. Dada T, Mohan S, Sihota R, et al. Comparison of ultrasound biomicroscopic parameters after laser

iridotomy in eyes with primary angle closure and primary angle closure glaucoma. Eye 2007;21:956–961.

16. He M, Friedman DS, Ge J, et al. Laser peripheral iridotomy in eyes with narrow drainage angles: ultrasound biomicroscopy outcomes. The Liwan Eye Study. Ophthalmology 2007;114:1513–1519.

17. Yao B-Q, Wu L-L, Zhang C, Wang X. Ultrasound biomicroscopic features associated with angle closure in fellow eyes of acute primary angle closure after laser iridotomy. Ophthalmology 2009;116:444–448.e2.

18. Gazzard G, Friedman DS, Devereux JG, et al. A prospective ultrasound biomicroscopy evaluation of changes in anterior segment morphology after laser iridotomy in Asian eyes. Ophthalmology 2003;110:630–638.

19. Lee KS, Sung KR, Kang SY, et al. Residual anterior chamber angle closure in narrow-angle eyes following laser peripheral iridotomy: anterior segment optical coherence tomography quantitative study. Jpn J Ophthalmol 2011;55:213–219.

20. Quigley HA. Long-Term Follow-up of Laser Iridotomy. Ophthalmology 1981;88:218–224.

21. Pollack IP. Laser iridotomy in the treatment of angle-closure glaucoma. Ann Ophthalmol 1981;13:549–550.

22. Friedman DS. Who needs an iridotomy? Br J Ophthalmol 2001;85:1019–1021.

23. How AC, Baskaran M, Kumar RS, et al. Changes in anterior segment morphology after laser peripheral iridotomy: an anterior segment optical coherence tomography study. Ophthalmology 2012;119:1383–1387.

24. Lee RY, Kasuga T, Cui QN, et al. Association between baseline iris thickness and prophylactic laser peripheral iridotomy outcomes in primary angle-closure suspects. Ophthalmology 2014;121:1194–1202.

25. Foster PJ, Buhrmann R, Quigley HA, Johnson GJ. The definition and classification of glaucoma in prevalence surveys. Br J Ophthalmol 2002;86:238–242.

26. Shaffer RN. Primary glaucomas. Gonioscopy, ophthalmoscopy and perimetry. Trans Am Acad Ophthalmol Otolaryngol 1960;64:112–127.

27. Liu S, Li H, Dorairaj S, et al. Assessment of scleral spur visibility with anterior segment optical coherence tomography. J Glaucoma 2010;19:132–135.

28. Mak H, Xu G, Leung CK-S. Imaging the iris with swept-source optical coherence tomography: relationship between iris volume and primary angle closure. Ophthalmology 2013;120:2517–2524.

29. Liu S, Yu M, Ye C, et al. Anterior chamber angle imaging with swept-source optical coherence tomography: an investigation on variability of angle measurement. Invest Ophthalmol Vis Sci 2011;52:8598–8603.

30. Lee RY, Kasuga T, Cui QN, et al. Association between baseline angle width and induced angle opening following prophylactic laser peripheral iridotomy. Invest Ophthalmol Vis Sci 2013;54:3763–3770.

31. Yoong Leong JC, O'Connor J, Soon Ang G, Wells AP. Anterior Segment Optical Coherence Tomography Changes to the Anterior Chamber Angle in the Short-term following Laser Peripheral Iridoplasty. J Curr

Glaucoma Pract 2014;8:1–6.

32. Ang BCH, Nongpiur ME, Aung T, et al. Changes in Japanese eyes after laser peripheral iridotomy: an anterior segment optical coherence tomography study. Clin Experiment Ophthalmol 2016;44:159–165.

33. Ng WT, Morgan W. Mechanisms and treatment of primary angle closure: a review. Clin Experiment Ophthalmol 2012;40:e218–28.

34. He M, Lu Y, Liu X, et al. Histologic changes of the iris in the development of angle closure in Chinese eyes. J Glaucoma 2008;17:386–392.

35. Oka N, Otori Y, Okada M, et al. Clinical study of anterior ocular segment topography in angle-closure glaucoma using the three-dimensional anterior segment analyzer Pentacam. europepmc.org 2006. Available at: http://europepmc.org/abstract/med/16764322.

36. Coakes RL, Lloyd-Jones D, Hitchings RA. Anterior chamber volume. Its measurement and clinical application. Trans Ophthalmol Soc U K 1979;99:78–81.

37. Dorairaj S, Liebmann JM, Ritch R. Quantitative evaluation of anterior segment parameters in the era of imaging. Trans Am Ophthalmol Soc 2007;105:99–108; discussion 108–10.

38. Radhakrishnan S, Goldsmith J, Huang D, et al. Comparison of optical coherence tomography and ultrasound biomicroscopy for detection of narrow anterior chamber angles. Arch Ophthalmol 2005;123:1053–1059.

Tables

Table 1. Baseline demographics and ocular examination.

Male	M 13 (31.7%)
Female	F: 28 (68.2%)
Age	58.6 ± 8.7
CCT	538 ± 29
Angle opening	0. 7 ± 0.4
IOP	13 ± 2.7
Axial length	22.5 ± 1.2

Table 2: The unadjusted univariate and adjusted multivariate linear regression for factors associated with increased anterior opening distance

		Unadjusted*				Adjusted**			
		Regression Coefficient	95% CI		P	Regression Coefficient	95% CI		P
			Lower	Upper			Lower	Upper	
ΔAOD_500	Age	0	0	0.01	0.375	0	0	0.01	0.249
	gender	0.05	-0.06	0.16	0.346	0.06	-0.04	0.16	0.257
	LV	-0.09	-0.51	0.34	0.681	0.17	-0.06	0.4	0.147
	cACD	-0.16	-0.72	0.4	0.562	-0.13	-0.28	0.01	0.072
	Iris volume	-0.01	-0.02	0	0.141	-0.01	-0.02	0	**0.022**
	IT2000	0.04	-0.04	0.12	0.35	0.001	<0.001	0.002	0.232
	ACV	-0.04	-0.08	0.01	0.03	-0.01	-0.01	0	**0.036**
ΔTISA_500	Age	0	0	0.01	0.366	0	0	0.01	0.193
	gender	-0.07	-0.15	0.01	0.081	-0.06	-0.15	0.03	0.19
	LV	-0.12	-0.44	0.21	0.466	0.08	-0.13	0.3	0.442
	cACD	-0.05	-0.47	0.38	0.827	-0.12	-0.25	0.01	0.06
	Iris volume	-0.01	-0.02	0	**0.007**	-0.01	-0.02	-0.01	**0.001**
	IT2000	0.01	-0.05	-0.05	0.756	<0.001	<0.001	0.001	0.363
	ACV	0	-0.04	0.03	0.83	-0.01	-0.01	0	**0.4**
ΔAOD_750	Age	0	-0.01	0.01	0.863	0	-0.01	0.01	0.622
	gender	0.08	-0.08	0.23	0.304	0.1	-0.04	0.24	0.161
	LV	0.07	-0.55	0.68	0.826	0.28	-0.04	0.59	0.084
	cACD	-0.16	-0.96	0.65	0.694	-0.17	-0.37	0.02	0.083
	Iris volume	-0.01	-0.02	0.01	0.336	-0.01	-0.02	0	0.103
	IT2000	-0.01	-0.04	0.01	0.206	0.001	<0.001	0.002	0.245
	ACV	-0.06	-0.32	0.2	0.653	-0.07	-0.14	0.01	**0.048**
ΔTISA_750	Age	0	0	0.01	0.315	0	0	0	0.291
	gender	0.04	-0.02	0.11	0.188	0.05	-0.01	0.11	0.125
	LV	-0.05	-0.32	0.23	0.728	0.13	-0.01	0.28	0.074
	cACD	-0.18	-0.54	0.17	0.305	-0.09	-0.18	0	0.06
	Iris volume	0	-0.01	0	0.258	-0.01	-0.01	0	**0.04**
	IT2000	0.03	-0.03	0.08	0.325	<0.001	<0.001	0.001	0.173
	ACV	-0.31	-0.82	0.19	0.215	-0.42	-0.83	0	**0.041**

Figures

Figure 1

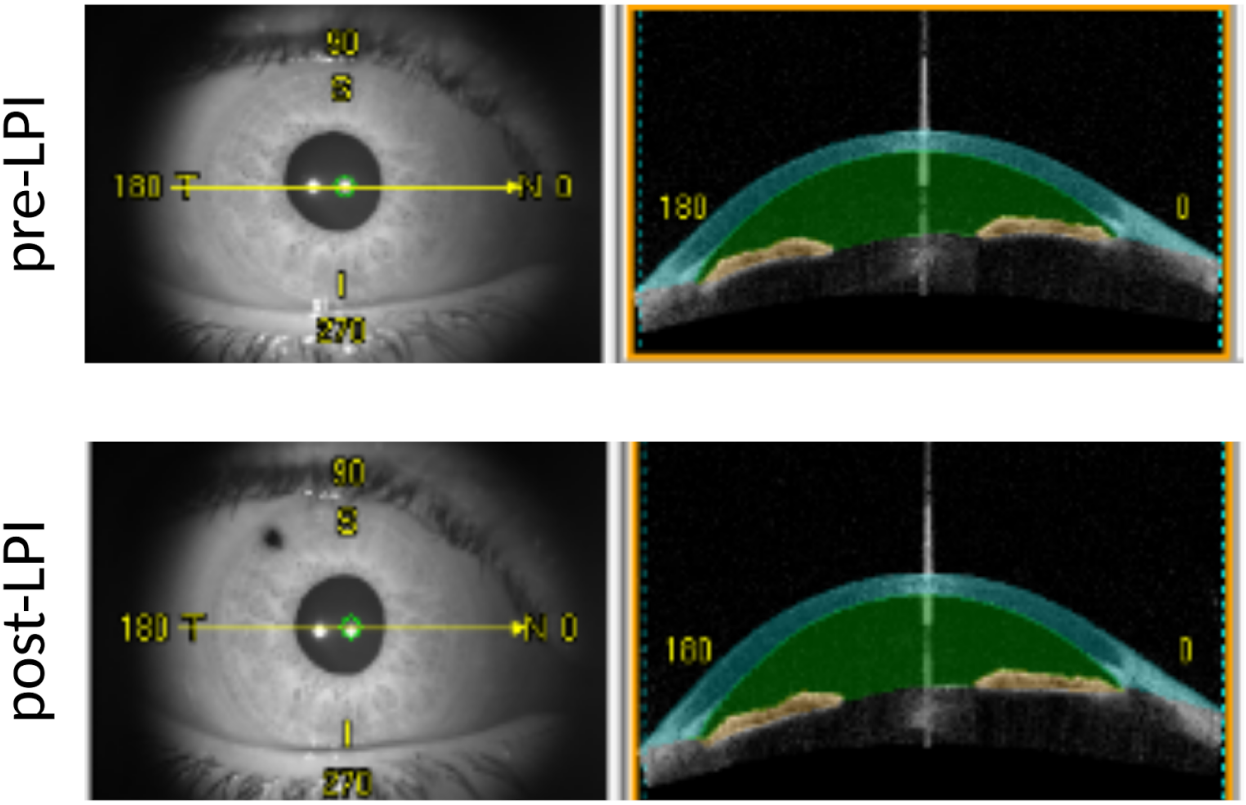

Figure 1: Anterior chamber measurements. Sixty-four anterior segment cross-sectional images of 128 angle meridians were analyzed. Instrument software automatically detected anterior and posterior surface of the iris (yellow color) and calculated iris volume. Anterior chamber volume increased from 111.84 mm ^{3} at the baseline (upper row) to 121.34 mm^3 post-LPI. (Lower row)**.**

Figure 2

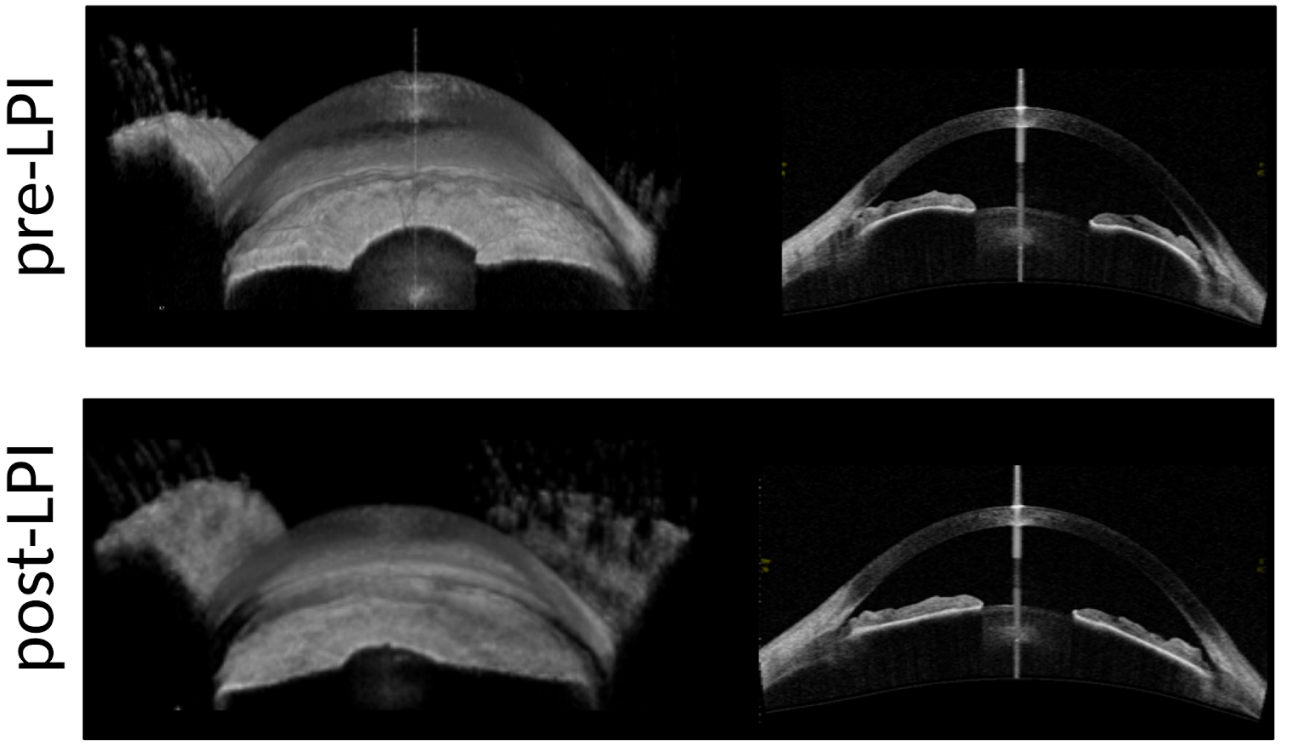

Figure 2: Iris volume was calculated by summing up of pixel volumes derived from each B-scan image. Before the LPI, iris had high curvature as evident by 3D-image of the iris (upper left) and cross sectional image of the iris (lower left). Iris resumes a more flat configuration after the LPI. (3D- upper right and cross-sectional lower right images).

Figure 3

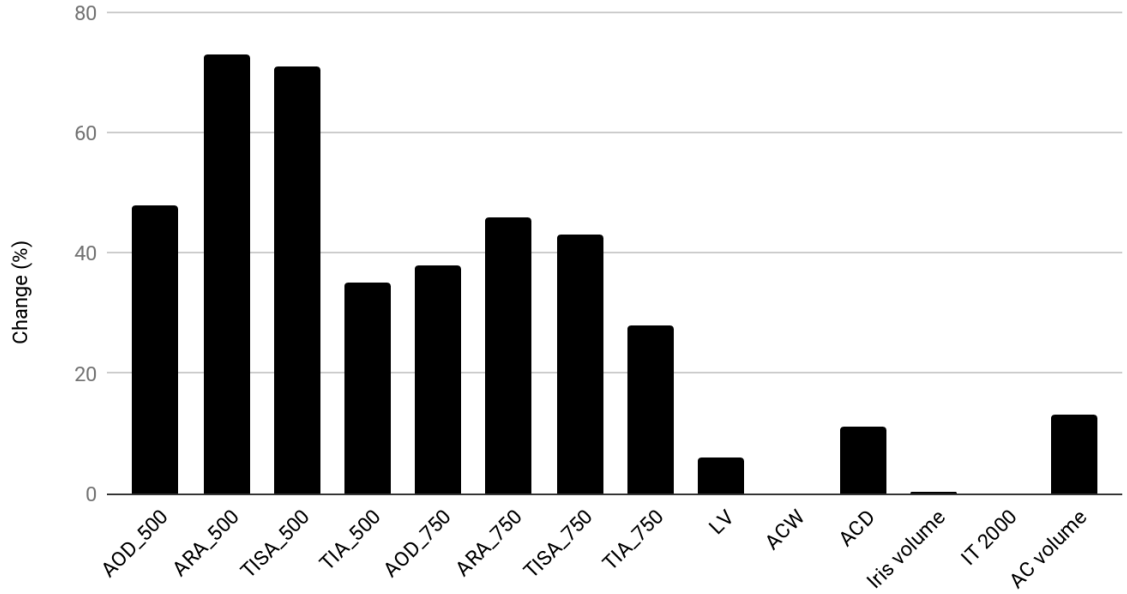

Figure 3: Changes in Mean Anterior Segment variables. Only LV, ACW, Iris volume and IT 2000 did not change significantly ($p>0.05$). AOD angle opening distance at 500 and 750 microns; ARA angle recess area at 500 and 750 microns; TISA: trabecular iris surface area; TIA: trabecular iris angle; ACD: anterior chamber depth; ACV: anterior chamber volume; ACW: anterior chamber width; LV lens vault; IT2000 iris thickness 2000 micron from the scleral spur.

Supplementary Table 1: Mean Anterior Segment variables before and after LPI

	Pre		Post		Change			
	Mean ± SD	**95% CI**	**Mean ± SD**	**95% CI**	**Mean ± SD**	**95% CI**	**%**	**P†**
AOD_500	0.38 ± 0.14	0.34 to 0.41	0.51 ± 0.16	0.47 to 0.55	0.13 ± 0.12	0.1 to 0.16	48	<0.001
ARA_500	0.21 ± 0.09	0.19 to 0.24	0.28 ± 0.11	0.25 to 0.31	0.07 ± 0.08	0.05 to 0.09	73	<0.001
TISA_500	0.15 ± 0.05	0.13 to 0.16	0.21 ± 0.09	0.18 to 0.22	0.06 ± 0.08	0.03 to 0.08	71	<0.001
TIA_500	22.6 ± 7.2	20.9 to 24.4	28.7 ± 7.1	26.9 to 30.4	6.1 ± 5.5	4.7 to 7.4	35	<0.001
AOD_750	0.52 ± 0.16	0.48 to 0.56	0.68 ± 0.19	0.63 to 0.72	0.16 ± 0.15	0.12 to 0.19	38	<0.001
ARA_750	0.33 ± 0.12	0.3 to 0.36	0.44 ± 0.15	0.4 to 0.47	0.11 ± 0.11	0.08 to 0.13	46	<0.001
TISA_750	0.26 ± 0.09	0.24 to 0.28	0.34 ± 0.11	0.32 to 0.37	0.08 ± 0.08	0.06 to 0.1	43	<0.001
TIA_750	24.4 ± 6.6	22.8 to 26	29.9 ± 6.7	28.2 to 31.5	5.5 ± 5.1	4.2 to 6.7	28	<0.001
LV	0.27 ± 0.19	0.23 to 0.32	0.26 ± 0.21	0.21 to 0.31	-0.02 ± 0.11	-0.04 to 0.01	6	0.761
ACW	10.9 ± 0.5	10.7 to 11	10.89 ± 0.45	10.78 to 11	0 ± 0.1	0 to 0.1	0	0.067
ACD	2.34 ± 0.38	2.25 to 2.43	2.42 ± 0.33	2.34 to 2.5	0.08 ± 0.31	0.01 to 0.16	11	0.001
Iris volume	28.2 ± 5	26.9 to 29.4	28.7 ± 5	27.5 to 30	0.5 ± 3.3	-0.27 to 1.35	0.3	0.755
AC volume	106 ± 25.6	99.7 to 112.3	118.8 ± 24.8	112.7 to 124.9	12.8 ± 8.1	10.8 to 14.8	13	<0.001
IT 2000	459 ± 34	451 to 468	458 ± 35	449 to 466	-1.15 ± 2.88	-1.86 to -0.44	0	<0.071

† Based on Paired t-test. ACA anterior chamber area; ACD anterior chamber depth; ACV anterior chamber volume; ACW anterior chamber width; AOD angle opening distance; ARA angle recess area; LV lens vault; SD standard deviation; TISA trabecular iris surface area.